
IMPROVING (α, f) -BYZANTINE RESILIENCE IN FEDERATED LEARNING VIA LAYERWISE AGGREGATION AND COSINE DISTANCE

Mario García-Márquez, Nuria Rodríguez-Barroso

Department of Computer Science and Artificial Intelligence,
Andalusian Research Institute in Data Science
and Computational Intelligence (DaSCI)
University of Granada
Granada
{mariogmarq, rbnuria}@ugr.es

M.V. Luzón

Department of Software Engineering,
Andalusian Research Institute in Data Science
and Computational Intelligence (DaSCI)
University of Granada
Granada
luzon@ugr.es

Francisco Herrera

Department of Computer Science and Artificial Intelligence,
Andalusian Research Institute in Data Science
and Computational Intelligence (DaSCI)
University of Granada
Granada
herrera@decsai.ugr.es

ABSTRACT

The rapid development of artificial intelligence systems has amplified societal concerns regarding their usage, necessitating regulatory frameworks that encompass data privacy. Federated Learning (FL) is posed as potential solution to data privacy challenges in distributed machine learning by enabling collaborative model training without data sharing. However, FL systems remain vulnerable to Byzantine attacks, where malicious nodes contribute corrupted model updates. While Byzantine Resilient operators have emerged as a widely adopted robust aggregation algorithm to mitigate these attacks, its efficacy diminishes significantly in high-dimensional parameter spaces, sometimes leading to poor performing models. This paper introduces Layerwise Cosine Aggregation, a novel aggregation scheme designed to enhance robustness of these rules in such high-dimensional settings while preserving computational efficiency. A theoretical analysis is presented, demonstrating the superior robustness of the proposed Layerwise Cosine Aggregation compared to original robust aggregation operators. Empirical evaluation across diverse image classification datasets, under varying data distributions and Byzantine attack scenarios, consistently demonstrates the improved performance of Layerwise Cosine Aggregation, achieving up to a 16% increase in model accuracy.

Keywords Federated Learning · Robust Aggregation · Machine Learning · Krum

1 Introduction

The rapid proliferation of Artificial Intelligence (AI) technologies has garnered significant societal and regulatory interest. The European Union AI Act [1] serves as a prominent example of this regulatory response, underscoring the need to address the application of AI systems, particularly within high-risk domains. Recognizing the still unclear understanding of the broader societal impacts of AI, the concept of trustworthy AI [2] has emerged as a critical paradigm. Trustworthy AI is based on the foundational principles of ethics, legality, and technical robustness. Specifically, trustworthy AI is implemented adhering to seven interconnected requirements: (1) human agency and oversight, (2) robustness and safety,

(3) privacy and data governance, (4) transparency, (5) diversity and non-discrimination, (6) social and environmental well-being, and (7) accountability.

Addressing the critical challenges of privacy and data governance, within the framework of regulations such as the GDPR [3], Federated Learning (FL) [4, 5] has gained recognition as a robust and increasingly adopted solution. FL employs a distributed learning mechanism. This mechanism facilitates collaborative model training across multiple clients, avoiding the need for direct data sharing, and consequently preserving client privacy during both training and deployment. However, it is crucial to acknowledge that despite these intrinsic privacy guarantees, FL is still susceptible to adversarial manipulations that can compromise data and model integrity.

Byzantine attacks pose a significant threat to the robustness and security of FL systems. Although considerable academic effort has been directed to address this vulnerability [6, 7, 8], a fundamental contribution in this area is the concept of (α, f) -Byzantine resilience [9]. Based on this foundation, numerous robust aggregation operators have been proposed [9, 10, 11, 6]. However, recent investigations have revealed that several of these operators exhibit susceptibility to attacks, particularly in high-dimensional scenarios [12, 13]. Furthermore, comparative evaluations suggest that the empirical performance of these robust operators is often suboptimal compared to less robust aggregation techniques, such as FedAvg [9, 10]. This performance gap raises concerns regarding their practical applicability in real-world Federated Learning deployments.

This study undertakes an investigation into the (α, f) -Byzantine resilience properties of well-established aggregation operators, including Krum, Bulyan, and GeoMed [9, 10]. Furthermore, it introduces a novel aggregation scheme specifically designed to address their limitations when applied to high-dimensional data. High-dimensional settings are often subject to the challenges associated with the curse of dimensionality, where substantial variations in a limited number of coordinates may result in only marginal changes in the overall vector magnitude or distance relative to other vectors. To mitigate this issue, the study proposes leveraging layerwise aggregation to decompose the aggregation problem into more manageable, lower-dimensional sub-problems, facilitating a more efficient and magnitude-sensitive aggregation process. Furthermore, inspired by the demonstrated success of cosine similarity (and consequently, cosine distance) in sparse, high-dimensional contexts [14], this research explores the substitution of Euclidean distance with cosine distance, premised on the rationale that it produces comparable data ordering when applied to normalized data. The proposed Layerwise Cosine aggregation rule scheme, which integrates both layerwise aggregation and cosine distance, demonstrably outperforms the conventional application of baseline operators in terms of both empirical performance and theoretical robustness, while maintaining its core properties. Importantly, this performance enhancement is achieved without introducing additional computational overhead, making the proposal a compelling and resource-efficient alternative to existing baseline operators.

To evaluate the efficacy of the proposed methodology, a comprehensive suite of image classification experiments was conducted utilizing the EMNIST, Fashion-MNIST, CIFAR-10, and CelebA-S datasets. The experimental design incorporated both Independent and Identically Distributed (IID) and non-IID data distributions across the simulated client population. Consistent with the established evaluation paradigm for the robust operators, the primary focus of this assessment was directed towards Byzantine attack scenarios. A comprehensive analysis was performed comparing the original operators, namely Krum [9], Bulyan [10] and GeoMed [10], their result of the Layerwise Cosine Aggregation scheme and its partial applications, aimed at empirically validating the anticipated performance enhancements. The empirical results show an improvement with respect to the baseline operator in every scenario showing up to 16% improved accuracy.

To assess the effectiveness of the proposed methodology, a comprehensive set of image classification experiments was performed, employing the EMNIST, Fashion-MNIST, CIFAR-10, and CelebA-S datasets. The experimental design encompassed both Independent and Identically Distributed (IID) and non-IID data distributions across the simulated client population. In accordance with the established evaluation paradigm for robust aggregation operators, the primary emphasis of this assessment was placed on Byzantine attack scenarios. A detailed comparative analysis was performed that evaluated the performance of the original operators, namely Krum [9], Bulyan [10] and GeoMed [10], along with the proposed layer-wise cosine aggregate scheme and its partial applications. This analysis aimed to empirically validate the anticipated performance gains. The empirical results demonstrate a consistent improvement over the baseline operators in all evaluated scenarios, with accuracy gains of up to 16% observed.

The subsequent sections of this paper are organized as follows. Section 2 provides the necessary background knowledge to follow the rest of the paper, including formal definitions of FL (Section 2.1), Byzantine attacks (Section 2.2), the notion of (α, f) -Byzantine resilience (Section 2.3), and some of the most popular robust operators (Section 2.4). The proposed aggregation scheme and its theoretical properties are presented in Section 3. Section 4 details the experiments performed, including a description of the datasets and models (Section 4.1), a description of the Byzantine attacks implemented (Section 4.2), the baselines used for comparison (Section 4.3) and additional relevant implementation details (Section 4.4). Section 5 provides a comparative analysis of the experimental results, considering two distinct

cases: the absence of adversarial clients (Section 5.1) and the presence of adversarial clients (Section 5.2). Finally, concluding remarks are presented in Section 6.

2 Background

This section aims to provide the background required to follow the rest of the work.

2.1 Federated Learning

FL is a distributed machine learning paradigm in which multiple entities collaborate to train a global model without explicitly exchanging data, preserving the privacy of each entity [4]. FL operates in two distinct phases:

1. **Training Phase.** In this phase, each client shares information derived from their local data, without revealing the raw dataset itself, to jointly train a machine learning model. This resulting global model may be stored on a single server, a designated client, or distributed among the clients.
2. **Inference Phase.** In this phase, clients collaborate to apply the collaboratively learned model to new instances.

Both phases can be performed synchronously or asynchronously, depending on various factors such as client availability. Formally [5], an FL scenario can be modeled as follows. We consider a set of n clients or data owners, denoted by $\{C_1, \dots, C_n\}$, where each client C_i possesses a local dataset D_i . Each client C_i also maintains a local model L_i , parameterized by weights $V_i \in \mathbb{R}^d$. The primary objective of FL is to train a global model G by leveraging the local datasets of the clients through an iterative process, to which each iteration is called a round of learning.

In a given round t , each client trains its local model using its local dataset D_i^t , resulting in a local model L_i^t with updated parameters V_i^t . These parameters V_i^t are then shared with a central parameter server to compute the global model G^{t+1} . The global model’s parameters are computed from aggregating the distinct local parameters V_1^t, \dots, V_n^t using a predefined aggregation function Δ . Formally, the global model’s parameters V_G^{t+1} are computed as:

$$V_G^{t+1} = \Delta(V_1^t, \dots, V_n^t). \quad (1)$$

Subsequently, the local model L_i^{t+1} is set to the global model G^{t+1} for every client i . This process is repeated until a predefined stopping criterion is met. Upon termination, the global model G encapsulates the knowledge learned from all individual clients.

2.2 Byzantine Attacks

FL, as a specialized instance of machine learning, inherits the susceptibility of its parent field to adversarial attacks that seek to degrade performance or compromise privacy. The existing literature categorizes these attacks through several criteria [6], including the attacker’s knowledge of the system, the manipulation of model behavior, and the attack’s objective. Within the latter taxonomy, untargeted attacks aim solely to reduce the model’s performance on the primary learning task. A particularly challenging case of this attack is the Byzantine attack [15, 16], in which a subset of clients submit arbitrary updates. These updates are typically generated randomly or derived from models trained on manipulated data, effectively producing random updates.

These attacks are frequently used in conjunction with model replacement techniques [17]. This is due to the fluctuating proportion of adversarial clients, which can prevent the mitigation of malicious updates, as the sheer number of benign client updates may not effectively counteract the influence of compromised updates.

2.3 Byzantine resilience

The prevalence of Byzantine attacks has motivated extensive research to improve the resilience of FL systems against these malicious intrusions. Many studies concentrate on the deployment of defensive strategies against Byzantine attacks on the server, particularly within the aggregation operator used to compute the parameters of the global model [6]. A fundamental question is to establish the conditions under which an aggregation operator or rule can be considered robust against Byzantine attacks. In this context, the most widely used definition is that of a (α, f) -Byzantine Resilient rule [9], detailed in Definition 1.

Definition 1. Let $\alpha \in [0, \frac{\pi}{2}]$ be any angle and $f \in \{1, \dots, n-1\}$ any integer. Let $n \in \mathbb{N}$, $V_i \in \mathbb{R}^d$ with $1 \leq i \leq n-f$ be independent, identically distributed vectors, with $V_i \sim G$ with $\mathbb{E}G = g$. Let $B_k \in \mathbb{R}^d$ with $n-f+1 \leq k \leq n$

be random vectors, possibly dependent between them and the vectors V_i 's. An aggregation rule \mathcal{F} is said to be (α, f) -Byzantine resilient if, for any $1 \leq j_1 \leq \dots \leq j_f \leq n$, the vector:

$$F = \mathcal{F}(V_1, \dots, B_1, \dots, B_f, \dots, V_n)$$

satisfies (i) $\langle \mathbb{E}F, g \rangle \geq (1 - \sin \alpha) \|g\|^2$ and (ii) for $r \in \{2, 3, 4\}$, $\mathbb{E}\|F\|^r$ is bounded by linear combinations of terms of the form $\mathbb{E}\|G\|^{r_1} \cdot \dots \cdot \|G\|^{r_{n-1}}$ with $r_1 \cdot \dots \cdot r_{n-1} = r$.

We will not dive into the theoretical details of this definition, but one can intuitively see it that given f Byzantine vectors, the expected output of the rule should deviate no more than an angle α from the true gradient. The second condition stated in the definition is required to transfer the dynamics of convergence of SGD to the operator [9, 18]. Also, note that α and f may vary between rules, thus giving us also a sense of how robust a rule may be compared to other.

2.4 Robust Aggregation Rules

The notion of (α, f) -Byzantine Robustness has been widely adopted in the literature as a basis for developing new robust aggregation rules. In particular, the Krum aggregation operator [9] stands out as the rule most frequently encountered in this body of work, and importantly, it was the operator that originally established the definition of (α, f) -Byzantine Robustness. The Krum operator, KR , is defined as:

$$KR(V_1, \dots, V_n) = \arg \min_{i \in \{1, \dots, n\}} s(i)$$

where $s(i)$ is defined as

$$s(i) = \sum_{i \rightarrow j} \|V_i - V_j\|^2.$$

Here, f is an hyperparameter to be taken into account, which denotes the expected amount of Byzantine vectors in the updates set. The original paper [9] proves the theoretical Byzantine resistance when $f < \frac{n}{2} - 1$.

Other common rules fundamented upon this definition include Bulyan [10] and GeoMed [10, 19]. Bulyan is a robust aggregation rule designed to enhance resilience against Byzantine attacks in distributed systems and federated learning. It operates through a two-step process: first, a subset of updates is selected using Krum, favoring those least affected by outliers or malicious contributions. Then, a coordinate-wise trimmed mean is applied to the selected updates, eliminating extreme values to produce a robust aggregated result. GeoMed is an aggregation rule inspired by the Geometric Median [19]. To address the high computational cost of the Geometric Median, GeoMed instead selects the medoid of the updates. The medoid is the point within a dataset that minimizes the sum of distances to all other data points. Although not formally proven to be an (α, f) -Byzantine resilient rule, GeoMed is considered a strong candidate and is frequently treated as such in the literature [10].

3 Layerwise Cosine aggregation rule

This section introduces the Layerwise Cosine aggregation rule concept, our proposed approach to improve (α, f) -Byzantine Resilient Rules while sustaining their robustness. We begin by outlining the limitations of specific operators in Section 3.1. Following this, we detail our proposal and perform a rigorous theoretical analysis of the Byzantine resilience of the Layerwise Cosine aggregation rule scheme in Section 3.2.

3.1 Limitations of operators

Byzantine resilient operators, such as Krum or Bulyan, are widely employed in FL due to their ability to enhance resilience against Byzantine attacks [6]. However, it is increasingly acknowledged that these methods can suffer from a reduced performance compared to alternatives such as FedAvg, especially when applied to high-dimensional models [9]. Recent investigations [12] have specifically highlighted the vulnerability of Krum, and, by extension, derived approaches such as Bulyan, to attacks that exploit high dimensionality. In these scenarios, operators may struggle to effectively identify subtle but critical adversarial manipulations spread across many dimensions.

A clear example of the challenges facing these aggregation operators arises in the context of aggregation of computational neural networks (CNNs). CNNs naturally exhibit an imbalance in the number of parameters across different layers, with convolutional layers typically having fewer parameters than dense layers. This parameter imbalance can distort the weighting process in algorithms for these operators. The result can be a misalignment between the actual importance of

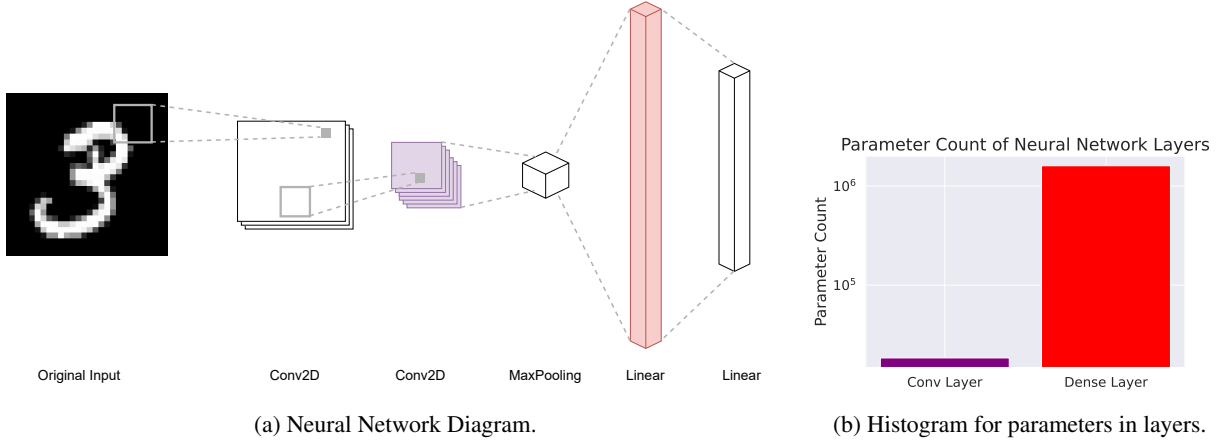


Figure 1: Parameter Distribution across Layers in a Two-Layer CNN used in some of the experiments. This figure highlights the significant parameter imbalance inherent in a basic two-layer CNN. A histogram directly compares the parameter count of the second convolutional layer (purple) and the first dense layer (red), revealing an order of magnitude difference. This disparity underscores the typical parameter distribution imbalance in such architectures. Detailed architectural specifications are provided in Section 4.4.

each layer to the network’s overall performance and the weight assigned by the aggregation operator, which tends to be skewed by the sheer number of parameters in a layer. A visual example of this problem can be seen in Figure 1.

Furthermore, even when dealing with architectures that do not exhibit significant parameter imbalances across layers, such as within Dense layers or Multilayer Perceptrons, aggregation rules like Krum and GeoMed often operate on data that exhibit sparsity. This sparsity introduces a notable difficulty because Euclidean distance, the fundamental metric used in Krum’s selection and conceptually related to GeoMed’s medoid choice, is not ideally suited for capturing meaningful distances within sparse data representations [14].

3.2 Layerwise Cosine Aggregation

In this section we will introduce our proposal, Layerwise Cosine Aggregation, a framework for improving robust aggregation rules, and provide theoretical results that our proposal is (α, f) -Byzantine Resilient under the same conditions as the original rules. This result indicates that the improvements made to any Byzantine Resilient operator lead to a valid robust aggregation rule for Byzantine learning.

Proposition 1 formally proves that the layerwise application of an (α, f) -Byzantine Resilient rule, also satisfies the criteria for Byzantine Resilience. From the proof of this proposition we infer that the bound shown in condition (i) of Definition 1 is improved over the original rule.

Subsequently, we explain how replacing the Euclidean distance within a given operator with the cosine distance, in conjunction with median gradient clipping, also results in a (α, f) -Byzantine resilient rule.

Therefore, to address the limitations mentioned above, we propose a novel approach, **Layerwise Cosine Aggregation**, which uses layer-wise aggregation to enhance the robustness of the given operator in conjunction with cosine distance and median gradient clipping. As illustrated in Figure 2, this approach decomposes the aggregation process into a series of layerwise sub-problems, effectively reducing the dimensionality of the parameter space considered by the original operator. By adopting a layer-wise strategy, we ensure that the robust operator accurately weights each layer based on its true contribution to model utility, rather than being influenced by the number of parameters within that layer.

Furthermore, even with the decomposition of the problem into subproblems, these subproblems may still present challenges for the operator. This difficulty stems from the significant imbalance between the number of updates and the parameter count, leading to a scenario where updates populate only a small portion of the parameter space. The cosine distance (and cosine similarity) has demonstrated effectiveness in such circumstances [14]. However, given that the cosine distance does not consider the magnitudes of updates, we incorporate median gradient clipping to address this limitation. The clipping to the median of the norms is employed as it consistently resides within the benign set [12]. In particular, these enhancements introduce minimal additional computational overhead, requiring approximately equivalent memory and computational resources as the original chosen operator.

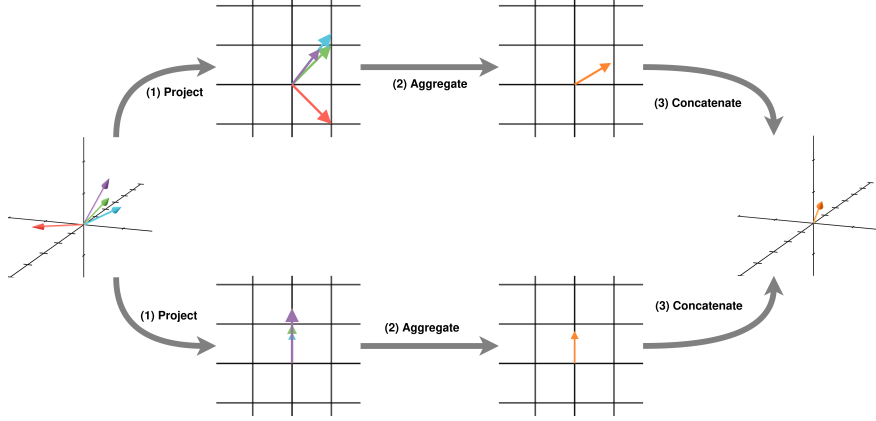


Figure 2: In a layerwise aggregation approach, original vectors are projected into orthogonal subspaces that partition the original space. Each set of projected vectors is then aggregated, and the resulting aggregated vectors are concatenated to produce a vector in the original space.

First, we will formally define the layer-wise application of a rule. Let $d = m_1 + \dots + m_k$. We will call k the numbers of layers. Given an aggregation rule \mathcal{F} , we define the layerwise application of \mathcal{F} , denoted by $L\mathcal{F}$, as

$$L\mathcal{F}(V_1, \dots, V_n) = (\mathcal{F}(V_{1,1}, \dots, V_{n,1}), \dots, \mathcal{F}(V_{1,k}, \dots, V_{n,k}))$$

where $V_{i,j}$ denotes the projection of the vector V_i to the j -th element of the partition $R^{m_1} \times \dots \times R^{m_k}$ of R^d .

Proposition 1. *The layerwise application of an (α, f) -Byzantine Resilient rule \mathcal{F} , $L\mathcal{F}$, is also an (α, f) -Byzantine Resilient rule.*

Proof. We will proceed by induction over the number of layers. For the first case, where the number of layers is 1, the result is direct by the fact that \mathcal{F} is (α, f) -Byzantine Resilient rule. Moving to the case with $n + 1$ layers. Let $\mathbb{E}G = g \in \mathbb{R}^{h+m}$ where h is the dimensionality of the parameters of the n first layers and m of the $n + 1$ -th layer. Let g_1 denote the projection of g into its first h coordinates and g_2 into his last m coordinates. Since \mathcal{F} is (α_m, f) -Byzantine Resilient and $L\mathcal{F}$ is (α, f) -Byzantine Resilient for the case of n layers, we have:

$$\begin{aligned} L\mathcal{F}(V_1, \dots, V_n) &= (L\mathcal{F}(V_{1,1}, \dots, V_{n,1}), \mathcal{F}(V_{1,2}, \dots, V_{n,2})) \\ &= (F_1, F_2) = F \end{aligned}$$

with the partition of $R^d = R^h \times R^m$. Then:

$$\langle \mathbb{E}F_1, g_1 \rangle \geq (1 - \sin \alpha_h) \|g_1\|^2.$$

For F_2 and g_2 one should change α_h by α_m . Considering $F = (F_1, F_2) \in \mathbb{R}^{h+m}$, we have

$$\begin{aligned} \langle \mathbb{E}F, g \rangle &= \langle \mathbb{E}F_1, g_1 \rangle + \langle \mathbb{E}F_2, g_2 \rangle \geq (1 - \sin \alpha) (\|g_1\|^2 + \|g_2\|^2) \\ &= (1 - \sin \alpha) \|g\|^2 \end{aligned}$$

where $\alpha = \max\{\alpha_h, \alpha_m\}$.

The second property can be render equivalent to the property $\mathbb{E}\|F\|^r \leq B_r + A_r \mathbb{E}\|G\|^r$ where A_r and B_r are scalars, with $r = 2, 3, 4$ [18, 10, 9]. We will proceed again by induction. The case of only one layer is again direct by the property that \mathcal{F} is (α, f) -Byzantine Resilient. Then, moving to the case of $n + 1$ and keeping notation of the previous part we have:

$$\begin{aligned} \mathbb{E}\|F\|^r &\leq \mathbb{E}\|F_1\|^r + \mathbb{E}\|F_2\|^r \\ &\leq (B_1 + A_1 \mathbb{E}\|g_1\|^r) + (B_2 + A_2 \mathbb{E}\|g_2\|^r) \\ &\leq (B_1 + A_1 \mathbb{E}\|G\|^r) + (B_2 + A_2 \mathbb{E}\|G\|^r) \\ &= (B_1 + B_2) + (A_1 + A_2) \mathbb{E}\|G\|^r. \end{aligned}$$

□

Now, we remember that the cosine distance between two vector V_j and V_i is defined as the $1 - \cos \theta_{ij}$ where θ_{ij} denotes the angle form by the two vectors. A well-known result indicates that for normalized data points, ($\|V_i\| = \|V_j\|$ for every i and j), similar to the data that we obtain after clipping, Euclidean and cosine distances exhibit a monotonic relationship [20]. This monotonicity implies that within normalized data, algorithms that use Euclidean distance to rank data points, for example by proximity, will produce equivalent rankings if cosine distance is used instead. Consequently, for distance-based aggregation operators like Krum, Bulyan, or GeoMed, replacing Euclidean distance with cosine distance should maintain their fundamental behavior and (α, f) -Byzantine Resilience. Despite this theoretical expectation of equivalence, it is plausible to anticipate empirical gains from employing cosine distance, as suggested by its successful application in areas such as vector embedding similarity [14] due to the sparsity of the update space.

Corollary 1. *The Layerwise Cosine Aggregation of an (α, f) -Byzantine Resilient rule which uses euclidean distance for ranking points, is also (α, f) -Byzantine Resilient.*

Proof. The proof is direct by applying Proposition 1 and taking into account the last paragraph. \square

An important result is that the Layerwise and Layerwise Cosine application of an operator may provide a better theoretical bound for the angle α than the original operator. Given (α, f) -byzantine resilient rule \mathcal{F} , its layer-wise application $L\mathcal{F}$ given a layer partition $d = m_1 + \dots + m_k$, takes α as $\max\{\alpha_{m_1}, \dots, \alpha_{m_k}\}$ where α_i is the α when \mathcal{F} is applied to data with dimension i . This result is derived from the proof of the byzantine robustness of $L\mathcal{F}$. In the case of Krum (and Bulyan), $\sin \alpha$ is directly proportional to the square root of the data dimension, and thus we are able to maximize the bound of the angle, providing a better theoretical robustness.

4 Experimental Setup

This section details the experimental setup designed to evaluate the robustness and effectiveness of the Layerwise Cosine Aggregation scheme. To evaluate the proposed method, we employed image classification models trained in various FL-optimized datasets. This section provides the necessary information to replicate our experimental environment, including the following. Section 4.1 outlines the datasets and models employed in each dataset, Section 4.2 introduces the label flipping attack, a Byzantine attack used in federated settings, Section 4.3 explains the baselines used in the experiments, and Section 4.4 provides specific implementation details. Our experimental design encompasses two distinct scenarios: evaluations conducted in the absence of adversarial clients and evaluations performed within a federated setting deliberately incorporating adversarial clients.

4.1 Dataset and models

For the evaluation of our proposal we have used classical image classification datasets. The datasets used and their federated distributions used are described as follows:

- **CIFAR-10.** This dataset is a labeled subset of the famous 80 million images dataset [21], consisting of 60,000 32x32 color images in 10 classes. The training data is evenly distributed between 200 clients.
- **Fashion MNIST.** This dataset [22] aims to be a more challenging replacement for the original MNIST dataset. It contains 28x28 grayscale clothing images from 10 different classes. We set the number of clients to 200.
- **EMNIST Non-IID.** This dataset, presented in 2017 in [23], is an extension of the MNIST dataset [24]. The EMNIST Digits class contains a balanced subset of the digits dataset. This dataset has been federated so that each client corresponds to the digits written by the same author, thus providing a real Non-IID federated setting.
- **EMNIST.** This dataset consists of the EMNIST data set, but where the training data have been federated following an IID distribution between 200 clients.
- **Celeba-S Non-IID.** The CelebA [25] dataset consists of famous face images with 40 binary attribute annotations per image. We use it as a binary image classification dataset, selecting a specific attribute as target, in particular, *Smiling*. We federate the dataset by assigning each famous person a client. Thus, the number of clients is set to more than 8000, but since some clients have a very poor dataset, we only considered clients with more than 30 samples in their local dataset, making the number of clients considered to be 1800.
- **Celeba-S.** This dataset consists on the Celeba-S dataset described above but where the data has been evenly distributed between 200 clients.

Regarding the models, we construct a convolutional neural network with 2 convolutional layers and 2 fully-connected layers as the global model for the Fashion MNIST, EMNIST and EMNIST Non-IID datasets. For the CIFAR-10, Celeba-S and Celeba-S Non-IID datasets, we use a pre-trained EffectiveNet-B0 [26] as the global model. Both models have been trained using an Adam optimizer with a learning rate of 0.001 and 10 epochs per round per client.

4.2 Label Flipping Byzantine attacks

For the poisoning attack, we consider a label-flipping-based attack. In this attack, the labels of a randomly selected subset of training data from adversarial clients are modified to contain a random label. This deliberate mislabeling causes adversarial clients to generate virtually random model updates, inducing a degradation in the performance of the global model.

This attack is often implemented in conjunction with a model replacement technique designed to amplify the impact of adversarial updates. Given a model parameter aggregation rule defined by the following equation:

$$V_G^{t+1} = V_G^t + \frac{\eta}{n} \sum_{i=1}^n (V_i^t - V_G^t) \quad (2)$$

where η represents the server learning rate (assumed to be one for the remainder of this work), an adversarial client may transmit the following update:

$$\hat{V}_{adv}^t = \beta(V_{adv}^t - V_G^t) \quad (3)$$

where $\beta = \frac{n}{\eta}$. Combining Equations 2 and 3, and assuming convergence of benign clients, yields the following approximation.

$$V_G^{t+1} \approx V_G^t + \frac{\eta}{n} \frac{n}{\eta} (V_{adv}^t - V_G^t) = V_{adv}^t.$$

4.3 Baselines

To empirically assess the efficacy of the Layerwise Cosine aggregation rule, we establish a set of baseline aggregation techniques for comparative analysis. We selected three well-established robust aggregation rules as baselines, namely Krum, Bulyan, and GeoMed, which are detailed in the following.

- **Krum** [9]: The Krum aggregation rule selects the update from the set of updates submitted $\{V_1, \dots, V_n\}$ that minimizes the sum of squared Euclidean distances to a subset of other updates. Formally, the Krum operator KR is defined as:

$$KR(V_1, \dots, V_n) = \underset{i \in \{1, \dots, n\}}{\operatorname{argmin}} s(i)$$

where the score function $s(i)$ is given by:

$$s(i) = \sum_{j \neq i} \|V_i - V_j\|^2$$

- **Bulyan** [10]: The Bulyan aggregation operator is based on the Krum selection process. It first computes the Krum score $s(i)$ for each update V_i . Subsequently, it selects a subset \mathcal{V} of m updates with the lowest Krum scores. The aggregated update is then computed as the average of the updates in this selected subset \mathcal{V} . Formally, the Bulyan operator B is defined as:

$$B(V_1, \dots, V_n) = \frac{1}{|\mathcal{V}|} \sum_{V \in \mathcal{V}} V$$

where $\mathcal{V} \subseteq \{V_1, \dots, V_n\}$ is the set of m updates with the lowest scores $s(i)$ as defined by the Krum operator. Following common practice, we set the hyperparameter m to 5 for our experiments.

- **GeoMed** [10, 19]: The Geometric Median (GeoMed) operator identifies the update within the set $\{V_1, \dots, V_n\}$ that minimizes the sum of squared Euclidean distances to all other updates in the set. The GeoMed operator Geo is defined as:

$$Geo(V_1, \dots, V_n) = \underset{V_j \in \{V_1, \dots, V_n\}}{\operatorname{argmin}} \sum_{i=1}^n \|V_i - V_j\|^2$$

Essentially, GeoMed selects the update that is centrally located with respect to the other submitted updates in terms of Euclidean distance.

For each of these baseline operators, we consider several variations to provide a comprehensive comparison. These variations include:

- **Original Operator:** The direct application of the standard Krum, Bulyan, or GeoMed operator as defined above.
- **Layerwise Application:** Applying each operator in a layer-wise manner. In this approach, the aggregation is performed independently for each layer of the neural network architecture utilized in the experiments.
- **Cosine Distance with Median Clipping:** Modifying the original operator by substituting the Euclidean distance metric with the cosine distance. Additionally, we incorporate median gradient clipping as a preprocessing step before aggregation when employing cosine distance, to further enhance robustness and maintain correct ordering.
- **Full Proposal (Layerwise Cosine):** The complete proposed scheme, which integrates both layerwise aggregation and the use of cosine distance in conjunction with median gradient clipping, applied to the chosen baseline operator.

This comprehensive set of baselines and their variations allows for a rigorous empirical evaluation of the proposed aggregation scheme.

4.4 Implementation details

To ensure reproducibility, we provide the code used to run all experiments ¹. The code is written using the FLEXible FL framework [27] ² and its companion library `flex-clash` ³ to simulate attacks on the FL scheme and access basic federated aggregation operators; also PyTorch [28] has been used for implementing the models.

5 Analysis of Results

In this section, we present a comprehensive analysis of the experimental results obtained to demonstrate the validity and robustness of the rules derived from the Layerwise Cosine Aggregation scheme as aggregation mechanisms. We will assess the effectiveness of the proposed method, focusing on test loss and accuracy in image classification models trained in various FL-adapted datasets. This analysis serves to validate the superiority of our Layerwise Cosine Aggregation proposal. We pay particular attention to the loss, examining its equivalence of results and its unbounded nature, which facilitates clearer analysis. The analysis is structured around two distinct scenarios explored in our experiments: the results obtained when no adversarial clients are present, analyzed in Section 5.1, and the results of federated settings under attack, explored in Section 5.2.

5.1 Analysis under no attack

The main results of the final test loss and accuracy achieved in the training under different operator variations are displayed in Table 1, Table 2 and Table 3, which displays the last test loss, the average of the test loss in the last 10 rounds, the minimum test loss achieved during the training, and the equivalent metrics for the accuracy for Krum, GeoMed and Bulyan, respectively. The results of the original operators are used as the baseline. However, to visualize the training process, the speed of convergence and mitigate the impact of potential overfitting, Figures 3, 4, and 5 illustrate the evolution of test loss during training rounds in relevant cases.

Across all six datasets, our proposed Layerwise Cosine Aggregation method consistently outperforms the standard operators, demonstrating improvements across all evaluated metrics. For example, on the Celeba-S Non-IID dataset, the Layerwise Cosine Krum achieves a substantial accuracy improvement exceeding 16%, while on CIFAR-10 the Layerwise Cosine Bulyan obtains an improvement over 12%. Furthermore, Figures 3 and 4 highlight a key advantage of our approach, particularly evident on the EMNIST Non-IID dataset. Here, the standard aggregators exhibit overfitting, characterized by an increasing test loss over communication rounds. In contrast, layerwise cosine aggregation and its partial applications effectively mitigate this overfitting. We attribute this superior performance to the significant

¹https://github.com/ari-dasci/S-layerwise_cosine_aggregation

²<https://github.com/FLEXible-FL/FLEXible>

³<https://github.com/FLEXible-FL/flex-clash>

parameter imbalance within the CNN model employed. Specifically, the first dense layer comprises 1.6 million parameters, while the initial convolutional layer contains only approximately 600. The potential overemphasis of the original operator on the dense layer may lead to model selection based primarily on the distribution of parameters within this layer, which may not be globally optimal. Layer-wise aggregation, by selectively aggregating updates for each layer, addresses this issue and yields improved results. Moreover, when selecting updates within the high-dimensional and sparse parameter space of the dense layer (100 samples in a space exceeding 1.6 million parameters), the cosine distance metric proves to be more effective than the Euclidean distance for comparing updates. Finally, our combined method, leveraging both layer-wise aggregation and cosine similarity, improves each individual technique, achieving the best overall performance.

This performance trend is consistent across the distinct datasets and operators. In cases with extreme parameter imbalance, such as the aforementioned example, Cosine Aggregation outperforms Layerwise aggregation. This likely occurs because even with layer separation, the dimensionality of the dense layer remains substantial, echoing the challenges faced by standard operators. Consequently, cosine distance proves to be more effective than layer-wise aggregation in such scenarios. In contrast, layer-wise aggregation emerges as a stronger option when using the EffectiveNet-B0 architecture. This network, while having a larger total number of parameters, distributes them across several layers. Therefore, layer-wise aggregation effectively reduces the dimensionality of each subproblem, improving performance compared to relying solely on cosine similarity. These results suggest that neither approach is universally superior. Rather, the combination of both techniques in Layerwise Cosine aggregation leverages the strengths of each, leading to impressive performance across diverse scenarios.

A notable exception to this general trend is observed in the case of Bulyan. As detailed in Table 3, the layer-wise aggregation exhibits a performance comparable to that of standard aggregation. In contrast, cosine aggregation demonstrates a significant improvement in all scenarios evaluated. We hypothesize that the enhanced performance of cosine aggregation can be attributed to its unique characteristic among the operators considered: it is the only method that employs multiple local updates in the computation of the global parameter. This increased information utilization may lead to a more balanced contribution from each layer, thereby replicating the performance advantages observed in layerwise aggregation.

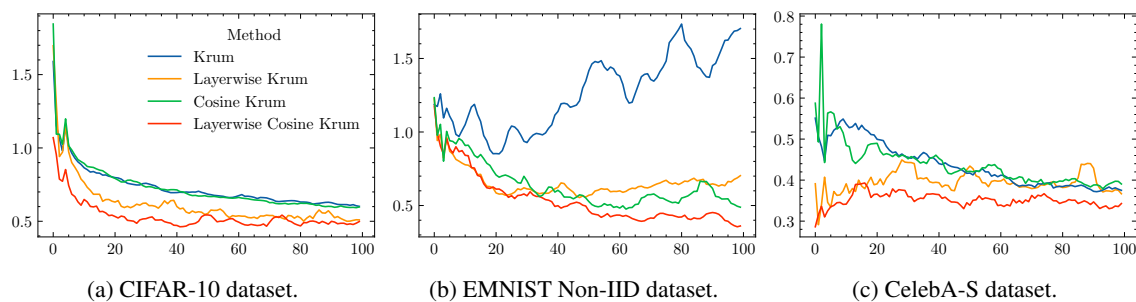


Figure 3: Test Loss in multiple image classification datasets depending on the training round for Krum.

Dataset	Method	Final Test Loss	Average Test Loss	Min. Test Loss	Average Test Accuracy	Max. Test Accuracy
CIFAR-10	Krum	0.584	0.608	0.584	0.844	0.844
	Layerwise Krum	0.505	0.509	0.457	0.865	0.870
	Cosine Krum	0.603	0.598	0.578	0.836	0.843
	Layerwise Cosine Krum	0.516	0.492	0.426	0.871	0.884
CelebA-S	Krum	0.373	0.377	0.361	0.913	0.917
	Layerwise Krum	0.352	0.370	0.291	0.920	0.920
	Cosine Krum	0.385	0.388	0.364	0.912	0.915
	Layerwise Cosine Krum	0.368	0.340	0.286	0.917	0.924
CelebA-S Non-IID	Krum	0.522	0.517	0.393	0.724	0.738
	Layerwise Krum	0.460	0.654	0.373	0.712	0.731
	Cosine Krum	0.475	0.469	0.363	0.870	0.895
	Layerwise Cosine Krum	0.408	0.426	0.317	0.885	0.907
EMNIST	Krum	0.244	0.244	0.087	0.984	0.985

	Layerwise Krum	0.062	0.064	0.059	0.987	0.988
	Cosine Krum	0.062	0.066	0.053	0.989	0.990
	Layerwise Cosine Krum	0.055	0.053	0.046	0.989	0.990
EMNIST	Krum	1.734	1.663	0.761	0.899	0.907
	Layerwise Krum	0.683	0.669	0.504	0.923	0.928
	Cosine Krum	0.477	0.517	0.416	0.936	0.944
Non-IID	Layerwise Cosine Krum	0.381	0.380	0.332	0.935	0.943
Fashion	Krum	1.648	1.706	0.626	0.852	0.859
	Layerwise Krum	0.613	0.604	0.491	0.870	0.874
	Cosine Krum	0.754	0.637	0.468	0.878	0.880
MNIST	Layerwise Cosine Krum	0.563	0.532	0.419	0.879	0.887

Table 1: Test Loss and Accuracy for every method under no attack for Krum.

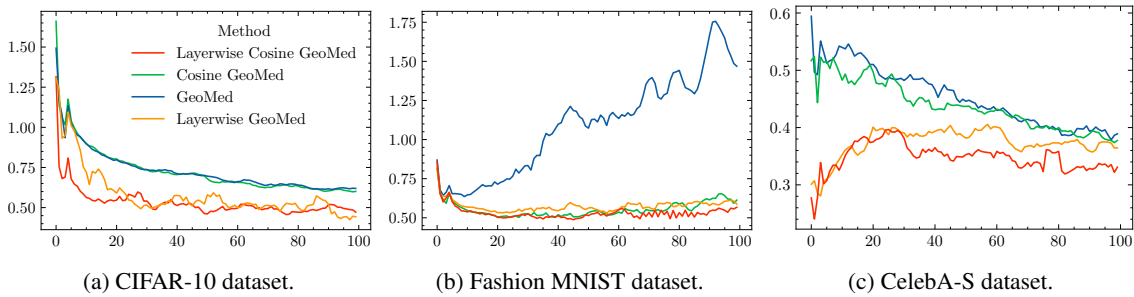


Figure 4: Test Loss in multiple image classification datasets depending on the training round for GeoMed.

Dataset	Method	Final Test Loss	Average Test Loss	Min. Test Loss	Average Test Accuracy	Max. Test Accuracy
CIFAR-10	GeoMed	0.621	0.621	0.594	0.837	0.840
	Layerwise GeoMed	0.425	0.437	0.375	0.877	0.892
	Cosine GeoMed	0.616	0.607	0.580	0.838	0.841
	Layerwise Cosine GeoMed	0.418	0.487	0.418	0.877	0.889
CelebA-S	GeoMed	0.401	0.391	0.361	0.913	0.916
	Layerwise GeoMed	0.364	0.370	0.281	0.918	0.922
	Cosine GeoMed	0.389	0.380	0.359	0.912	0.914
	Layerwise Cosine GeoMed	0.351	0.333	0.240	0.921	0.924
CelebA-S	GeoMed	0.409	0.528	0.382	0.871	0.891
	Layerwise GeoMed	0.661	0.575	0.322	0.853	0.892
	Cosine GeoMed	0.756	0.570	0.373	0.856	0.892
	Non-IID	Layerwise Cosine GeoMed	0.592	0.464	0.347	0.894
EMNIST	GeoMed	0.229	0.234	0.100	0.983	0.984
	Layerwise GeoMed	0.092	0.098	0.080	0.986	0.986
	Cosine GeoMed	0.068	0.064	0.051	0.989	0.990
	Layerwise Cosine GeoMed	0.055	0.050	0.046	0.990	0.991
EMNIST	GeoMed	2.670	2.018	0.729	0.891	0.907
	Layerwise GeoMed	0.725	0.643	0.476	0.931	0.936
	Cosine GeoMed	0.659	0.576	0.431	0.931	0.939
	Non-IID	Layerwise Cosine GeoMed	0.325	0.391	0.325	0.933
Fashion	GeoMed	1.496	1.579	0.604	0.855	0.860
	Layerwise GeoMed	0.538	0.590	0.482	0.869	0.872
	Cosine GeoMed	0.732	0.633	0.455	0.879	0.883
MNIST	Layerwise Cosine GeoMed	0.533	0.561	0.411	0.883	0.887

Table 2: Test Loss and Accuracy for every method under no attack for GeoMed.

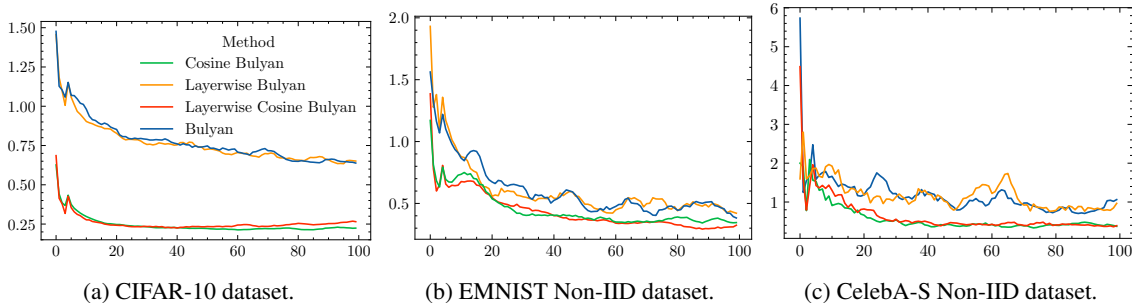


Figure 5: Test Loss in multiple image classification datasets depending on the training round for Bulyan.

Dataset	Method	Final Test Loss	Average Test Loss	Min. Test Loss	Average Test Accuracy	Max. Test Accuracy
CIFAR-10	Bulyan	0.641	0.643	0.622	0.828	0.833
	Layerwise Bulyan	0.628	0.644	0.616	0.828	0.831
	Cosine Bulyan	0.230	0.226	0.210	0.946	0.948
	Layerwise Cosine Bulyan	0.252	0.262	0.211	0.946	0.948
CelebA-S	Bulyan	0.405	0.388	0.367	0.910	0.915
	Layerwise Bulyan	0.378	0.379	0.361	0.912	0.914
	Cosine Bulyan	0.351	0.338	0.210	0.923	0.926
	Layerwise Cosine Bulyan	0.396	0.384	0.221	0.924	0.927
CelebA-S Non-IID	Bulyan	0.952	0.940	0.535	0.810	0.865
	Layerwise Bulyan	1.242	0.891	0.523	0.789	0.864
	Cosine Bulyan	0.264	0.388	0.264	0.901	0.913
	Layerwise Cosine Bulyan	0.471	0.388	0.308	0.902	0.914
EMNIST	Bulyan	0.057	0.057	0.051	0.989	0.990
	Layerwise Bulyan	0.057	0.054	0.048	0.989	0.990
	Cosine Bulyan	0.036	0.036	0.034	0.993	0.993
	Layerwise Cosine Bulyan	0.034	0.038	0.034	0.992	0.993
EMNIST Non-IID	Bulyan	0.360	0.423	0.311	0.930	0.945
	Layerwise Bulyan	0.411	0.446	0.341	0.930	0.942
	Cosine Bulyan	0.366	0.358	0.326	0.955	0.959
	Layerwise Cosine Bulyan	0.352	0.312	0.267	0.947	0.950
Fashion	Bulyan	0.491	0.495	0.452	0.882	0.885
	Layerwise Bulyan	0.460	0.497	0.433	0.881	0.885
	Cosine Bulyan	0.473	0.448	0.374	0.905	0.907
MNIST	Layerwise Cosine Bulyan	0.377	0.459	0.375	0.904	0.905

Table 3: Test Loss and Accuracy for every method under no attack for Bulyan.

5.2 Analysis under Byzantine attack

In the second scenario, where FL environments are subjected to adversarial attacks, the primary results are summarized in Tables 4, 5 and 6, showing the metrics for Krum, GeoMed and Bulyan respectively. Layerwise Cosine Aggregation, and its partial applications, consistently outperforms the baseline operators across all evaluated datasets. As depicted in Figures 6, 7 and 8 and by comparing these results tables in the previous section, our proposed method achieves performance comparable to that obtained in the absence of adversarial clients. This empirical evidence highlights the strong Byzantine robustness of Layerwise Cosine Aggregation.

While a detailed analysis of these results is provided in the previous scenario, it is crucial to reiterate the importance of gradient clipping within Layerwise Cosine Aggregation. Because cosine distance is sensitive to direction but not magnitude, it may incorrectly identify two updates with drastically different norms as similar. This can potentially compromise convergence by selecting updates with excessively large norms. This issue is particularly pronounced in settings employing the EfficientNet-B0 model, where high-norm updates in batch normalization layers can render the model ineffective. By incorporating median gradient clipping, we effectively focus on the gradient direction, mitigating this problem.

Therefore, and consistent with the results from the previous scenario, our proposed aggregation operator emerges as a more robust and effective choice in the presence of adversarial attacks.

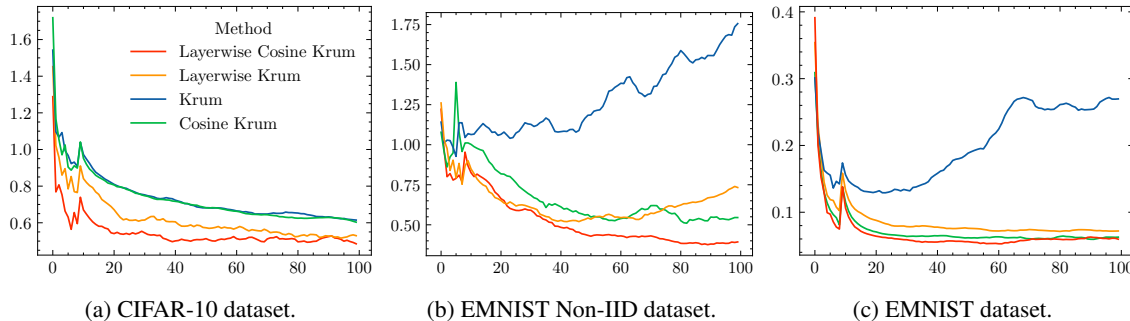


Figure 6: Test Loss under a Label Flipping attack depending on the training round for Krum.

Dataset	Method	Final Test Loss	Average Test Loss	Min. Test Loss	Average Test Accuracy	Max. Test Accuracy
CIFAR-10	Krum	0.598	0.615	0.591	0.836	0.840
	Layerwise Krum	0.496	0.530	0.463	0.860	0.871
	Cosine Krum	0.577	0.603	0.577	0.838	0.844
	Layerwise Cosine Krum	0.502	0.485	0.420	0.846	0.888
CelebA-S	Krum	0.379	0.389	0.365	0.914	0.917
	Layerwise Krum	0.364	0.379	0.289	0.917	0.921
	Cosine Krum	0.402	0.384	0.345	0.911	0.915
	Layerwise Cosine Krum	0.334	0.326	0.245	0.920	0.923
CelebA-S Non-IID	Krum	0.491	0.548	0.425	0.723	0.736
	Layerwise Krum	0.556	0.668	0.353	0.841	0.887
	Cosine Krum	0.772	0.548	0.350	0.857	0.896
	Layerwise Cosine Krum	0.531	0.456	0.338	0.887	0.902
EMNIST	Krum	0.268	0.270	0.115	0.982	0.983
	Layerwise Krum	0.074	0.072	0.066	0.987	0.987
	Cosine Krum	0.058	0.063	0.052	0.989	0.990
	Layerwise Cosine Krum	0.058	0.060	0.047	0.988	0.989
EMNIST Non-IID	Krum	1.911	1.756	0.756	0.903	0.911
	Layerwise Krum	0.708	0.733	0.461	0.927	0.931
	Cosine Krum	0.449	0.545	0.437	0.932	0.944
	Layerwise Cosine Krum	0.400	0.393	0.322	0.933	0.938
Fashion	Krum	1.434	1.764	0.641	0.849	0.854
	Layerwise Krum	0.642	0.653	0.492	0.865	0.869
	Cosine Krum	0.681	0.644	0.484	0.874	0.879
MNIST	Layerwise Cosine Krum	0.633	0.555	0.405	0.870	0.880

Table 4: Test Loss and Accuracy for every method under the label flipping attack for Krum.

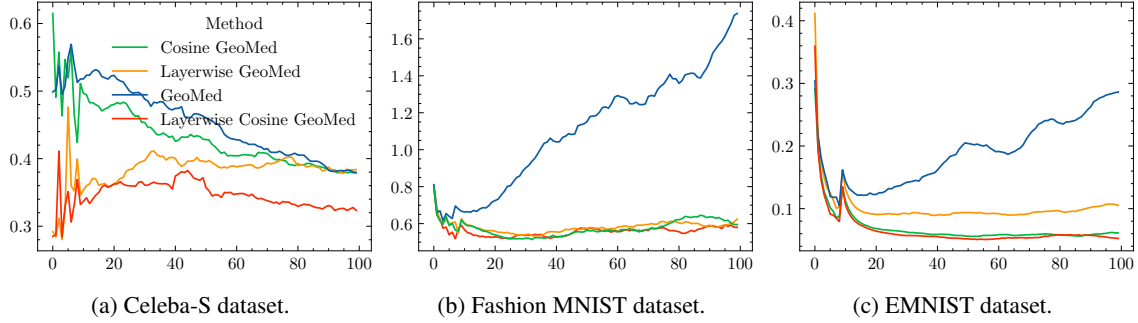


Figure 7: Test Loss under a Label Flipping attack depending on the training round for GeoMed.

Dataset	Method	Final Test Loss	Average Test Loss	Min. Test Loss	Average Test Accuracy	Max. Test Accuracy
CIFAR-10	GeoMed	0.598	0.607	0.587	0.838	0.841
	Layerwise GeoMed	0.585	0.499	0.399	0.865	0.881
	Cosine GeoMed	0.622	0.602	0.588	0.839	0.841
	Layerwise Cosine GeoMed	0.534	0.509	0.408	0.872	0.888
CelebA-S	GeoMed	0.374	0.379	0.356	0.913	0.917
	Layerwise GeoMed	0.385	0.384	0.280	0.918	0.919
	Cosine GeoMed	0.357	0.379	0.357	0.912	0.916
	Layerwise Cosine GeoMed	0.316	0.323	0.285	0.921	0.924
CelebA-S Non-IID	GeoMed	0.563	0.528	0.382	0.876	0.897
	Layerwise GeoMed	0.304	0.846	0.304	0.805	0.890
	Cosine GeoMed	0.493	0.571	0.386	0.858	0.890
	Layerwise Cosine GeoMed	0.456	0.444	0.319	0.897	0.911
EMNIST	GeoMed	0.297	0.286	0.105	0.982	0.983
	Layerwise GeoMed	0.095	0.105	0.078	0.985	0.986
	Cosine GeoMed	0.061	0.062	0.052	0.989	0.990
	Layerwise Cosine GeoMed	0.051	0.052	0.046	0.989	0.990
EMNIST Non-IID	GeoMed	1.165	1.654	0.772	0.897	0.910
	Layerwise GeoMed	0.555	0.598	0.476	0.927	0.937
	Cosine GeoMed	0.708	0.544	0.458	0.933	0.943
	Layerwise Cosine GeoMed	0.378	0.376	0.338	0.933	0.940
Fashion MNIST	GeoMed	1.707	1.737	0.600	0.851	0.858
	Layerwise GeoMed	0.758	0.625	0.500	0.867	0.871
	Cosine GeoMed	0.564	0.595	0.458	0.876	0.880
	Layerwise Cosine GeoMed	0.663	0.580	0.450	0.868	0.878

Table 5: Test Loss and Accuracy for every method under the label flipping attack for GeoMed.

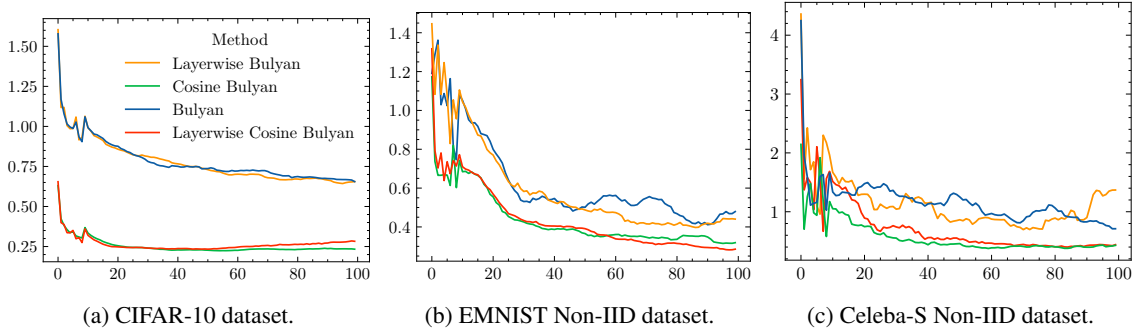


Figure 8: Test Loss under a Label Flipping attack depending on the training round for Bulyan.

Dataset	Method	Final Test Loss	Average Test Loss	Min. Test Loss	Average Test Accuracy	Max. Test Accuracy
CIFAR-10	Bulyan	0.648	0.655	0.637	0.826	0.829
	Layerwise Bulyan	0.655	0.655	0.626	0.827	0.831
	Cosine Bulyan	0.229	0.234	0.217	0.946	0.948
	Layerwise Cosine Bulyan	0.287	0.283	0.222	0.943	0.947
CelebA-S	Bulyan	0.373	0.386	0.364	0.910	0.915
	Layerwise Bulyan	0.410	0.411	0.371	0.911	0.914
	Cosine Bulyan	0.369	0.353	0.220	0.923	0.926
	Layerwise Cosine Bulyan	0.383	0.388	0.232	0.921	0.926
CelebA-S Non-IID	Bulyan	0.686	0.711	0.443	0.829	0.869
	Layerwise Bulyan	0.942	1.369	0.476	0.757	0.861
	Cosine Bulyan	0.415	0.429	0.260	0.904	0.915
	Layerwise Cosine Bulyan	0.513	0.440	0.322	0.899	0.916
EMNIST	Bulyan	0.042	0.056	0.042	0.989	0.990
	Layerwise Bulyan	0.060	0.059	0.051	0.989	0.990
	Cosine Bulyan	0.034	0.037	0.034	0.993	0.993
	Layerwise Cosine Bulyan	0.039	0.039	0.034	0.992	0.993
EMNIST Non-IID	Bulyan	0.570	0.479	0.316	0.929	0.941
	Layerwise Bulyan	0.443	0.440	0.321	0.932	0.942
	Cosine Bulyan	0.373	0.319	0.292	0.959	0.962
	Layerwise Cosine Bulyan	0.298	0.285	0.236	0.950	0.955
Fashion	Bulyan	0.536	0.501	0.455	0.882	0.885
	Layerwise Bulyan	0.481	0.476	0.428	0.883	0.886
	Cosine Bulyan	0.568	0.495	0.384	0.901	0.902
MNIST	Layerwise Cosine Bulyan	0.438	0.488	0.378	0.899	0.902

Table 6: Test Loss and Accuracy for every method under the label flipping attack for Bulyan.

6 Conclusions and Future Work

Due to the distributed nature of FL, mitigating Byzantine attacks has become a critical area of research. The introduction of (α, f) -Byzantine resilient operators represented a significant advancement in the field, both theoretically and empirically. However, with continued use, its limitations have become apparent. This work addresses these limitations by exploring the theoretical properties and proposing Layerwise Cosine aggregation rule, an improved aggregation scheme that introduces minimal computational overhead. The principal contributions of this work are as follows:

- Show, both theoretically and empirically, a discernible decrease in performance for robust aggregation rules based on (α, f) -Byzantine resilience when applied to high-dimensional data. This observation reveals a significant performance gap between robust and effective FL models in such settings, highlighting a critical challenge in the field.

- To propose the layer-wise aggregation, while preserving the theoretical properties of Byzantine resilience, allows us to derive a tighter theoretical bound on the expected angle, leading to improved robustness against Byzantine attacks.
- To combine layer-wise aggregation with the use of cosine distance, we obtain a theoretically and empirically significantly improved robust aggregation scheme for certain operators: Layerwise Cosine Aggregation.

Our findings demonstrate the broad applicability of our proposed scheme, exemplified by its successful enhancement of widely adopted operators such as Krum, Bulyan, and GeoMed. Across all scenarios studied, our approach consistently yielded performance improvements, indicating a promising step toward bridging robust and effective privacy-conscious training paradigms. This work also highlights the potential for revisiting the foundations of well-established methods, enabling significant improvements across multiple related areas.

Future Work. Although this study has demonstrated the effectiveness of Layerwise Cosine Aggregation in improving robustness under Byzantine scenarios within image classification tasks, several promising directions remain open for exploration. Future work may extend this framework to other data modalities such as natural language processing and time series forecasting, where high-dimensional and sparse representations are common. Furthermore, deploying and evaluating the method in real-world federated environments, where device availability, communication constraints, and heterogeneous hardware introduce further complexity, would offer valuable practical insights. Finally, exploring adaptive or learnable layer-wise distance metrics, beyond static cosine similarity, could further enhance the flexibility and effectiveness of the aggregation process across diverse neural architectures.

Acknowledgments

This research results of the Strategic Project IAFER-Cib (C074/23), as a result of the collaboration agreement signed between the National Institute of Cybersecurity (INCIBE) and the University of Granada. This initiative is carried out within the framework of the Recovery, Transformation, and Resilience Plan funds, financed by the European Union (Next Generation).

References

- [1] Council of European Union. Regulation of the european parliament and of the council laying down harmonised rules on artificial intelligence (artificial intelligence act) and amending certain union legislative acts, 2021.
- [2] Scott Thiebes, Sebastian Lins, and Ali Sunyaev. Trustworthy artificial intelligence. *Electronic Markets*, 31(2):447–464, Jun 2021.
- [3] European Parliament and Council of the European Union. Regulation (EU) 2016/679 of the European Parliament and of the Council.
- [4] Brendan McMahan, Eider Moore, Daniel Ramage, Seth Hampson, and Blaise Aguera y Arcas. Communication-Efficient Learning of Deep Networks from Decentralized Data. In Aarti Singh and Jerry Zhu, editors, *Proceedings of the 20th International Conference on Artificial Intelligence and Statistics*, volume 54 of *Proceedings of Machine Learning Research*, pages 1273–1282. PMLR, 2017.
- [5] M. Victoria Luzón, Nuria Rodríguez-Barroso, Alberto Argente-Garrido, Daniel Jiménez-López, Jose M. Moyano, Javier Del Ser, Weiping Ding, and Francisco Herrera. A tutorial on federated learning from theory to practice: Foundations, software frameworks, exemplary use cases, and selected trends. *IEEE/CAA Journal of Automatica Sinica*, 11(JAS-2023-0937):824, 2024.
- [6] Nuria Rodríguez-Barroso, Daniel Jiménez-López, M. Victoria Luzón, Francisco Herrera, and Eugenio Martínez-Cámara. Survey on federated learning threats: Concepts, taxonomy on attacks and defences, experimental study and challenges. *Information Fusion*, 90:148–173, 2023.
- [7] Yaru Zhao, Jianbiao Zhang, and Yihao Cao. Manipulating vulnerability: Poisoning attacks and countermeasures in federated cloud-edge-client learning for image classification. *Knowledge-Based Systems*, 259:110072, 2023.
- [8] Umer Zukaib and Xiaohui Cui. Mitigating backdoor attacks in federated learning based intrusion detection systems through neuron synaptic weight adjustment. *Knowledge-Based Systems*, 314:113167, 2025.
- [9] Peva Blanchard, El Mahdi El Mhamdi, Rachid Guerraoui, and Julien Stainer. Machine learning with adversaries: byzantine tolerant gradient descent. In *Proceedings of the 31st International Conference on Neural Information Processing Systems*, NIPS’17, page 118–128, Red Hook, NY, USA, 2017. Curran Associates Inc.

- [10] El Mahdi El Mhamdi, Rachid Guerraoui, and Sébastien Rouault. The hidden vulnerability of distributed learning in Byzantium. In Jennifer Dy and Andreas Krause, editors, *Proceedings of the 35th International Conference on Machine Learning*, volume 80 of *Proceedings of Machine Learning Research*, pages 3521–3530. PMLR, 10–15 Jul 2018.
- [11] Nuria Rodríguez-Barroso, Eugenio Martínez-Cámara, M. Victoria Luzón, and Francisco Herrera. Backdoor attacks-resilient aggregation based on robust filtering of outliers in federated learning for image classification. *Knowledge-Based Systems*, 245:108588, 2022.
- [12] Moran Baruch, Gilad Baruch, and Yoav Goldberg. *A little is enough: circumventing defenses for distributed learning*. Curran Associates Inc., Red Hook, NY, USA, 2019.
- [13] Jian Xu, Shao-Lun Huang, Linqi Song, and Tian Lan. Byzantine-robust federated learning through collaborative malicious gradient filtering. In *2022 IEEE 42nd International Conference on Distributed Computing Systems (ICDCS)*, pages 1223–1235, 2022.
- [14] Hugo Touvron, Thibaut Lavril, Gautier Izacard, Xavier Martinet, Marie-Anne Lachaux, Timothée Lacroix, Baptiste Rozière, Naman Goyal, Eric Hambro, Faisal Azhar, Aurelien Rodriguez, Armand Joulin, Edouard Grave, and Guillaume Lample. Llama: Open and efficient foundation language models, 2023.
- [15] Leslie Lamport, Robert Shostak, and Marshall Pease. The byzantine generals problem. *ACM Trans. Program. Lang. Syst.*, 4(3):382–401, July 1982.
- [16] Shengshan Hu, Jianrong Lu, Wei Wan, and Leo Yu Zhang. Challenges and approaches for mitigating byzantine attacks in federated learning. *2022 IEEE International Conference on Trust, Security and Privacy in Computing and Communications (TrustCom)*, pages 139–146, 2021.
- [17] Eugene Bagdasaryan, Andreas Veit, Yiqing Hua, Deborah Estrin, and Vitaly Shmatikov. How to backdoor federated learning. In Silvia Chiappa and Roberto Calandra, editors, *Proceedings of the Twenty Third International Conference on Artificial Intelligence and Statistics*, volume 108 of *Proceedings of Machine Learning Research*, pages 2938–2948. PMLR, 26–28 Aug 2020.
- [18] L Eon Bottou. Online learning and stochastic approximations. 1998.
- [19] Peter Rousseeuw. Multivariate estimation with high breakdown point. *Mathematical Statistics and Applications Vol. B*, pages 283–297, 01 1985.
- [20] Gang Qian, Shamik Sural, Yuelong Gu, and Sakti Pramanik. Similarity between euclidean and cosine angle distance for nearest neighbor queries. In *Proceedings of the 2004 ACM Symposium on Applied Computing, SAC '04*, page 1232–1237. Association for Computing Machinery, 2004.
- [21] Alex Krizhevsky. Learning multiple layers of features from tiny images. Technical report, 2009.
- [22] Han Xiao, Kashif Rasul, and Roland Vollgraf. Fashion-mnist: a novel image dataset for benchmarking machine learning algorithms. *CoRR*, 1708.07747, 2017.
- [23] Gregory Cohen, Saeed Afshar, Jonathan Tapson, and André van Schaik. Emnist: Extending mnist to handwritten letters. In *2017 International Joint Conference on Neural Networks (IJCNN)*, pages 2921–2926, 2017.
- [24] Y. Lecun, L. Bottou, Y. Bengio, and P. Haffner. Gradient-based learning applied to document recognition. *Proceedings of the IEEE*, 86(11):2278–2324, 1998.
- [25] Ziwei Liu, Ping Luo, Xiaogang Wang, and Xiaoou Tang. Deep learning face attributes in the wild. In *Proceedings of the IEEE international conference on computer vision*, pages 3730–3738, 2015.
- [26] Mingxing Tan and Quoc Le. EfficientNet: Rethinking model scaling for convolutional neural networks. In Kamalika Chaudhuri and Ruslan Salakhutdinov, editors, *Proceedings of the 36th International Conference on Machine Learning*, volume 97 of *Proceedings of Machine Learning Research*, pages 6105–6114, 2019.
- [27] Francisco Herrera, Daniel Jiménez-López, Alberto Argente-Garrido, Nuria Rodríguez-Barroso, Cristina Zuheros, Ignacio Aguilera-Martos, Beatriz Bello, Mario García-Márquez, and María Victoria Luzón. Flex: Flexible federated learning framework. *Information Fusion*, 117:102792, 2025.
- [28] Adam Paszke, Sam Gross, Francisco Massa, Adam Lerer, James Bradbury, Gregory Chanan, Trevor Killeen, Zeming Lin, Natalia Gimelshein, Luca Antiga, Alban Desmaison, Andreas Köpf, Edward Yang, Zach DeVito, Martin Raison, Alykhan Tejani, Sasank Chilamkurthy, Benoit Steiner, Lu Fang, Junjie Bai, and Soumith Chintala. Pytorch: An imperative style, high-performance deep learning library, 2019.